A Highly Sensitive, Dual-Readout Assay Based on Gold Nanoparticles for Organophosphorus and Carbamate Pesticides

ARTICLE *in* ANALYTICAL CHEMISTRY · APRIL 2012

Impact Factor: 5.64 · DOI: 10.1021/ac300545p · Source: PubMed

analytical chemistry

Article

pubs.acs.org/ac

A Highly Sensitive, Dual-Readout Assay Based on Gold Nanoparticles for Organophosphorus and Carbamate Pesticides

Dingbin Liu,[†,§] Wenwen Chen,[†,§] Jinhua Wei,[‡,§] Xuebing Li,[‡] Zhuo Wang,*[,†] and Xingyu Jiang*[,†]

[†]CAS Key Lab for Biological Effects of Nanomaterials and Nanosafety, National Center for Nanoscience and Technology, 11 Beiyitiao, Zhongguancun, Beijing 100190, China

[‡]Institute of Microbiology, Chinese Academy of Science, 8 North Second Street, Haidian District, Beijing 100190, China

[§]Graduate University of Chinese Academy of Sciences, Shijingshan, Yuquan Road 19A, Beijing 100049, China

Supporting Information

ABSTRACT: This report presents a highly sensitive, rhodamine B-covered gold nanoparticle (RB-AuNP) -based assay with dual readouts (colorimetric and fluorometric) for detecting organophosphorus and carbamate pesticides in complex solutions. The detection mechanism is based on the fact that these pesticides can inhibit the activity of acetylcholinesterase (AChE), thus preventing the generation of thiocholine (which turns the RB-AuNP solutions blue and unquenches the fluorescence of RB simultaneously). The color of the RB-AuNP solution remains red and the fluorescence of RB remains quenched. By use of this dual-readout assay, the lowest detectable concentrations for several kinds of pesticides including carbaryl, diazinon, malathion, and phorate were measured to be 0.1, 0.1, 0.3, and 1 μg/L, respectively, all of which are much lower than the maximum residue limits (MRL) as reported in the European Union pesticides database as well as those from the U.S. Department Agriculture (USDA). This assay allows detection of pesticides in real samples such as agricultural products and river water. The results in detecting pesticide residues collected from food samples via this method agree well with those from high-performance liquid chromatography (HPLC). This simple assay is therefore suitable for sensing pesticides in complex samples, especially in combination with other portable platforms.

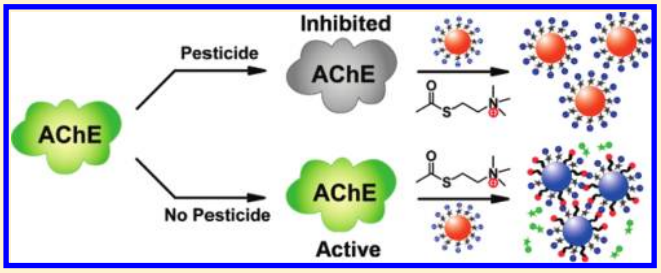

We provide a highly sensitive, dual-readout (colorimetric and fluorometric) assay for organophosphorus and carbamate pesticides in aqueous solutions and real samples. Foodborne illnesses are prevalent in both developed and developing countries. According to the World Health Organization, 1.5 billion cases of diarrhea in children (leading to more than 3 million deaths) are caused by contaminated food each year.[1] Food safety issues have therefore become the spotlight of public concerns all over the world. Organophosphorus compounds and carbamates are the most widely used pesticides in agriculture due to their relatively low persistence under natural conditions and high effectiveness for insect eradication. However, these pesticides exhibit acute toxicity on human health through their residues in agricultural products and contamination of water.[2−7] The high toxicity of organophosphorus and carbamate pesticides is ascribed to their ability to inhibit the activity of acetylcholinesterase (AChE), which is an essential enzyme to break down the neurotransmitter acetylcholine at cholinergic synapses. Inhibition of AChE activity allows acetylcholine to remain active in the synapse, thus leading to fatal consequences.[8−11] Therefore, it is important to develop highly sensitive and reliable probes for pesticides in complex samples.

In the past decade, many efforts have been made to develop efficient methods to determine pesticides in food or water. For instance, liquid/gas chromatography−mass spectrometry,[12,13] electrochemical analysis,[14−16] and enzyme-linked immunosorbent assays (ELISAs)[17] have been performed to detect pesticides. Although these methods have high selectivity and adequate sensitivity and allow discrimination of pesticides among complex samples, they either involve expensive biomolecule reagents, tedious pretreatment of samples, or/and require skilled operators and sophisticated instrumentation. Thus, these conventional methods are not suitable for on-site detection in most settings.

Recently, with the widespread development of nanoscience and technology, novel nanomaterials hold much potential to generate improved options for analysis on account of their unique chemical or physical properties.[18−21] For example, an optical sensor integrating CdTe semiconductor quantum dots (QDs) with AChE through layer-by-layer assembly was reported to sensitively detect organophosphorus pesticides in vegetables and fruits.[22] Carbon nanotubes exhibit superior electrocatalytic activity and thus have been employed for the determination of pesticides with ultrahigh sensitivity.[23] These

Received: February 23, 2012
Accepted: April 5, 2012
Published: April 5, 2012

   dx.doi.org/10.1021/ac300545p | Anal. Chem. 2012, 84, 4185−4191

probes, however, may induce environmental biosafety issues or require complicated procedures for synthesis.[24−27]

Gold nanoparticle (AuNP) -based colorimetric assays have recently become useful for many types of analytes without the need for advanced instruments because molecular events can be transformed into color changes.[28−33] The color changes are highly sensitive to the size, shape, capping agents, and medium refractive index, as well as the aggregation states of AuNPs, among which the modulation of aggregation states of AuNPs has been broadly used as a colorimetric assay for various analytes.[34] In general, solutions containing well-dispersed AuNPs display red color, while those containing aggregates of AuNPs exhibit purple or blue color. The color changes of AuNP solutions can be confirmed by the significant absorption band shift in the visible region of the electromagnetic spectrum.[28−33] Though the past decade has witnessed a variety of AuNP-based colorimetric assays for pesticides,[35−38] most of them still lack sufficient sensitivity, which significantly prevents this kind of assay from being transformed from proof-of-concept studies toward real-life analytical applications.[35,37,38] Therefore, to bring the AuNP-based assays into real world, a scheme to improve their sensitivity is necessary.

We recently designed a highly sensitive and selective rhodamine B-functionalized gold nanoparticle (RB-AuNP) -based assay with dual readouts (colorimetric and fluorometric) for monitoring the level of AChE in the cerebrospinal fluid of transgenic mice suffering from Alzheimer's disease.[39] Organophosphorus and carbamate pesticides represent two kinds of commonly used AChE inhibitors. Based on the inhibition of AChE activity, the probes for the determination of organophosphorus and carbamate pesticides have been intensely investigated due to their excellent sensitivity and selectivity. In this study, RB was applied as an ideal ligand because it provides water solubility, photostability, and strong fluorescence, and also because it readily adsorbs onto surfaces of AuNPs via electrostatic interactions to result in the quenching of its fluorescence. The addition of acetylthiocholine (ATC, an analogue of acetylcholine) and AChE into RB-AuNP solution leads to color change of the solutions from red to purple, simultaneously accompanied by the recovery of fluorescence of RB (initially quenched by AuNPs). This phenomenon is based on the fact that AChE can hydrolyze ATC to generate thiocholine, which can bind more strongly onto surfaces of AuNPs than RB, thus removing RB from the Au surface to recover the fluorescence of RB. Meanwhile, thiocholine and the residual RB attached onto different AuNP surfaces are able to recognize via electrostatic interaction, causing the aggregation of AuNPs, which is reflected by the color change of AuNP solution from red to purple quickly. If AChE is pretreated with AChE inhibitors such as organophosphorus compounds or carbamates, these pesticides can inhibit AChE activity, thus preventing the generation of thiocholine from the hydrolysis of ATC catalyzed by AChE. As a consequence, the color of the RB-AuNPs solutions remains red and the fluorescence of RB molecules remains quenched (Scheme 1). By contrast, other components in real samples are unable to impede the AChE-induced red-to-purple color change or fluorescence recovery. Owing to its much better sensitivity than those previously reported,[35−38] this present dual-readout assay can thereby be a reliable option to determine pesticides in food and water.

Scheme 1. Design of the Dual-Readout (Colorimetric and Fluorometric) Assay for Pesticides[a]

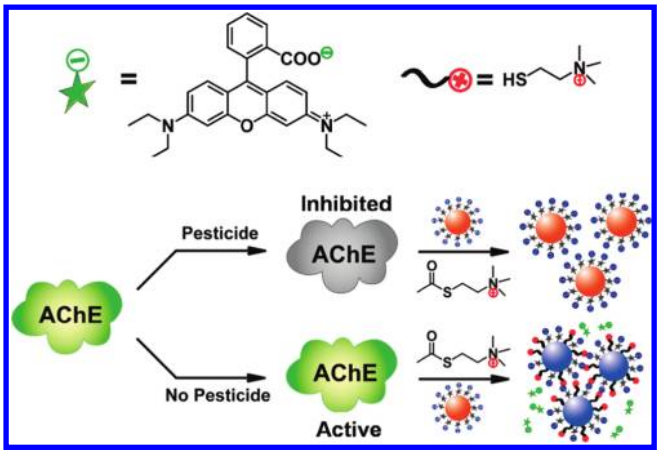

[a]AChE can catalyze ATC to produce thiocholine, thus causing the color of RB-AuNP solutions to change from red to blue, accompanied by fluorescence recovery of RB (the color of the stars changed from gray to green). The presence of pesticides can inhibit the activity of AChE, thus blocking the hydrolysis of ATC. No generation of thiocholine keeps the color of the RB-AuNP solutions red, and the fluorescence of RB remains quenched by AuNPs.

EXPERIMENTAL SECTION

Materials and Instrumentation. All chemicals were purchased from major suppliers such as Alfa Aesar and Sigma−Aldrich and were used as received. UV−vis spectra were recorded with a UV2450 spectrophotometer (Shimadzu). The fluorescence spectra were collected on a Hitachi F-4500 fluorescence spectrophotometer operating at an excitation wavelength at 550 nm; excitation and emission slit widths were 10 and 12 nm, respectively. The fluorescence intensities were collected at 575 nm. Dynamic light scattering (DLS) and zeta potential (ζ) were performed on a Zeta Sizer Nano ZS (Malvern Zetasizer 3000HS and He/Ne laser at 632.8 nm at scattering angles of 90 at 25 °C). Transmission electron microscopy (TEM) images were obtained by using a JEOL1400 model at an accelerating voltage of 100 kV. Fluorescent images were taken on a Leica inverted microscope with a charge-coupled device (CCD). High-performance liquid chromatography (HPLC) analysis was performed on a RP-HPLC column (Synergi Hydro-RP80A, 250 mm × 4.6 mm i.d., 4 μm), which was protected by a guard column (KJO-4282, 12.5 mm × 4.6 mm i.d., 4 μm). A mixture of acetonitrile−water (80:20 v/v) was used as an isocratic mobile phase to deliver the samples containing RB molecules at a flow rate of 1 mL/min at 28 °C, and their UV absorbance at 550 nm was recorded; while acetonitrile−water (60:40 v/v) was used as the isocratic mobile phase to deliver the food samples containing carbaryl at a flow rate of 1 mL/min at 28 °C, and their UV absorbance at 280 nm was recorded. Apple juice and spiked food solutions were prepared with a juice extractor (Philips, HR2006, 350 W) bought from a supermarket.

Preparation of Solutions. A stock solution of ATC (10 mM) was freshly prepared in double-distilled water and not used for more than 3 h after preparation to minimize possible hydrolysis. Both organophosphorus compounds (diazinon, malathion, and phorate) and carbamates (carbaryl) were initially dissolved in methanol to a relatively high concentration (1 g/L), which was later diluted at least 100-fold with double-

dx.doi.org/10.1021/ac300545p | Anal. Chem. 2012, 84, 4185−4191

distilled water. In the resulting solutions, such low levels of organic solvent have been shown to have negligible effects on the activity of AChE. Phosphate-buffered saline (PBS) was used to dissolve AChE (1 unit/μL), which was diluted with distilled water and used immediately for the following experiments.

Preparation of Citrate-Capped AuNPs (13 nm). Citrate-capped AuNPs were prepared according to the literature.[39,40] Briefly, a stirred aqueous solution of $HAuCl_4$ (41 mg, 1.0 mM) in 100 mL of water was heated to reflux, and a trisodium citrate solution (114 mg, 38.8 mM) dissolved in hot water (10 mL) was added. The solution was heated under reflux with vigorous stirring for another 15 min, during which its color changed from pale yellow to deep red. The solution was cooled to room temperature with a slow and continuous stir. The resulting solution was filtered with a polyethersulfone (PES) membrane (filter unit is 22 μm) to remove some large clusters and insoluble compounds. The sizes of the nanoparticles were about 13 nm by TEM analysis; the corresponding absorption band is at ~520 nm.

Preparation of RB-AuNPs. The preparation of RB-AuNPs was reported in previous work.[39,41] Briefly, a stock solution of RB (2 mM, 0.6 μL) was added with stirring into solutions of the as-prepared 13 nm citrate-AuNPs (5 nM, 1.0 mL), which were prepared in 2.5 mM $NaHCO_3$–NaOH buffer (pH 10.0). The resulting solutions were stirred mildly in the dark at room temperature for 2 h. The fluorescence spectra of the RB-AuNP solutions were measured with excitation at 550 nm. The very weak fluorescence of RB-AuNP solutions indicated that nearly all the RB molecules had absorbed onto the surfaces of AuNPs and the fluorescence was strongly quenched by AuNPs.

Experimental Procedure for the Sensitivity of This Assay. To aliquots of AChE (10 milliunits/mL) solution were added various amounts of carbaryl (final concentrations were set to be 0, 0.1, 0.3, 0.6, 1.0, 3.0, 6.0, 10, and 100 μg/L). To each mixture was added RB-AuNPs (0.5 mL, 5 nM), and then aliquots of ATC (20 μM) were finally added into the mixtures. The resulting mixtures were kept in the dark for 5 min, the pictures were taken, and at the same time, UV–vis absorption and fluorescence were measured respectively. All the measurements were repeated six times for each concentration, and the relationships between the percentage enzyme inhibition and the concentrations of pesticides were plotted as calibration curves, which were used to calculate their IC_{50} values.

Analysis of Carbaryl in River Water and Apple Juice. River water was collected from the Tangxun River, one of the tributaries of the Yangtze River. Apple juice was chosen as the fruit matrix to evaluate the potential of this assay for pesticides in real-world applications. The apples were first chopped and the edible parts of the apples were crushed into a homogenate by a juice extractor. Twenty-five grams of the apple homogenate was mixed with 25 mL of methanol, and the resulting mixture was filtered through a PES membrane (filter unit is 22 μm) to remove the insoluble materials. Different volumes of carbaryl methanol solutions (1 g/L) were mixed with the above-mentioned river water and apple juice, respectively, to result in final concentrations of carbaryl of 0, 0.01, 0.1, 1, 10, and 100 mg/L (10 mL of each concentration). Five microliters of each solution was first incubated with AChE (10 milliunits/mL) at 37 °C for 30 min, and then RB-AuNPs (0.5 mL, 5 nM) and ATC (20 μM) were finally added into the mixtures. UV–vis absorption and fluorescence were measured respectively after 5 min of incubation in the dark.

Measurement of Carbaryl Residues in Food Samples. We used tomatoes (350 g) and cucumbers (350 g) as the food sample matrix to investigate carbaryl residue levels with time. A carbaryl solution (100 mg/L) was sprayed on the skins of tomatoes and cucumbers, respectively, and then stored at room temperature overnight. The carbaryl-spiked tomatoes and cucumbers were washed and then left outdoors. The samples were prepared in 1, 2, 3, 4, 5, 6, and 7 days by the procedure outlined above, that is, the samples were chopped and their edible parts were crushed into a homogenate by the juice extractor. Each homogenate was mixed with methanol for a final volume of 10 mL. The carbaryl residues were measured by this dual-readout assay as described above.

RESULTS AND DISCUSSION

Mechanism of the Dual-Readout Assay for Pesticides. We first synthesized RB-AuNPs by allowing an optimized concentration of RB (1.2 μM) to adsorb on the surfaces of citrate-AuNPs (5 nM), which were initially prepared in 2.5 mM $NaHCO_3$–NaOH buffer (pH 10.0). The absorption band of RB-AuNPs was similar to that of the citrate-AuNPs, and in the meantime, the color of RB-AuNP solution remained red. We reasoned that the positively charged amino groups on RB molecules can readily absorb onto the negatively charged citrate-AuNPs via electrostatic interaction, thus leading to the mostly quenched fluorescence of RB by AuNPs.[39] Upon the addition of both ATC and AChE into a RB-AuNP solution, the quenched fluorescence of the RB molecules recovered significantly, accompanied with the change of color from red to purple of the RB-AuNPs solutions (Figure 1a). In order to evaluate the potential of this dual-readout assay for pesticides, AChE (10 mU/mL) was initially incubated with carbaryl (an AChE inhibitor used as a conventional carbamate pesticide) (1 mg/L) at 37 °C for 30 min, and then RB-AuNPs (0.5 mL, 5 nM) and ATC (20 μM) were added into the mixture in sequence. We found that the color of the mixed solution remained red even after 30 min of standing, while those without pretreatment of carbaryl changed from red to purple immediately. Moreover, the pretreatment of carbaryl prevented the fluorescence recovery of RB molecules, while those without pretreatment of carbaryl liberated intense fluorescence. These phenomena are attributed to the fact that carbaryl is capable of inhibiting AChE activity, thus preventing the generation of thiolcholine arising from the AChE-catalyzed hydrolysis of ATC.[42,43] As a result, the absence of thiolcholine can induce

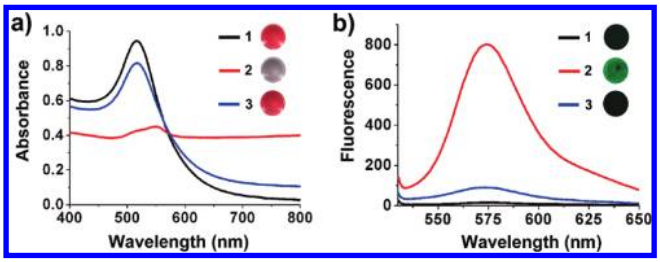

Figure 1. (a) UV–vis absorption and color changes of RB-AuNP solutions and (b) their corresponding fluorescence spectra and fluorescence images. 1, RB-AuNP solution; 2, RB-AuNP solution that was incubated with AChE and ATC; 3, RB-AuNP solution containing AChE was pretreated with carbaryl (100 μg/L), and ATC was added finally. The concentraion of AChE was standardized to be 1 unit/mL, and that of ATC was 20 μM.

dx.doi.org/10.1021/ac300545p | Anal. Chem. 2012, 84, 4185–4191

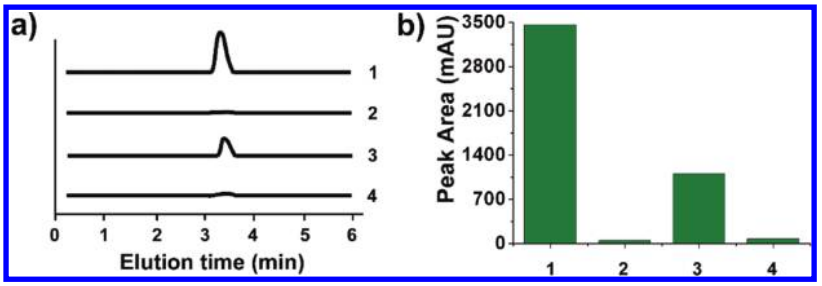

Figure 2. (a) Free RB molecules in solutions were measured by reverse-phase HPLC. (b) Amounts of free RB molecules were quantified by calculating their peak areas from the HPLC analysis. RB molecules (2 mM, 0.6 μL) before (trace 1) and after (trace 2) incubation with citrate-AuNPs (5 nM, 1.0 mL) are shown; RB molecules were partially released from surfaces of RB-AuNPs after incubation with AChE and ATC (trace 3), and that containing AChE was pretreated with carbaryl (100 μg/L) and then added ATC (trace 4). The concentraion of AChE was standardized to be 1 unit/mL, and that of ATC was 20 μM.

neither color change of RB-AuNP solutions nor fluorescence recovery of RB, which was confirmed by UV−vis absorption and fluorescence spectra. As shown in Figure 1a, with the carbaryl pretreatment, the absorption band of RB-AuNPs had few changes, while that of the sample without addition of carbaryl underwent significant changes. At the same time, the detached RB molecules from Au surfaces were detected by fluorescence spectroscopy (Figure 1b). The carbaryl pretreatment that prevented the fluorescence recovery of RB confirmed the fact that carbaryl inhibited AChE activity.

Characterizations to Support the Detection Mechanism. To further demonstrate the proposed mechanism, ζ potential measurements were first performed to investigate the changes of the surface charge of RB-AuNPs. The charge on RB-AuNPs was negative because of the carboxyl group on RB. The charge of aggregated RB-AuNPs was neutralized to a certain degree by the presence of thiocholine derived from AChE-catalyzed hydrolysis of ATC. We found the ζ potential of well-dispersed RB-AuNPs and that of the AChE-induced aggregates of RB-AuNPs were around −40 and 0.6 mV, respectively, while the ζ potential of those pretreated with carbaryl was −34.9 mV, which was close to that of the well-dispersed RB-AuNPs (Figure S1, Supporting Information). The inhibition process was also supported by dynamic light scattering (DLS) data (Figure S2, Supporting Information). The average hydrodynamic diameter of well-dispersed RB-AuNPs and that of the AChE-induced aggregates of RB-AuNPs were around 21 and 400 nm, respectively, while those pretreated with carbaryl had a diameter around 27 nm. The changes of aggregation states of RB-AuNPs were congruent with TEM analysis (Figure S3, Supporting Information), confirming the fact that these pesticides were capable of preventing the aggregation of RB-AuNPs as well as the fluorescence recovery of RB molecules.

The amounts of free RB molecules were analyzed by high-performance liquid chromatography (HPLC) with a UV−vis absorption detector. As shown in Figure 2a, the free RB molecules exhibited a monodisperse peak at an elution time of 3.3 min (trace 1), which disappeared upon the addition of citrate-AuNPs (trace 2) into RB solution, indicating the absorption of RB molecules onto citrate-AuNPs. Next, the RB-AuNP solution was incubated with AChE (1 unit/mL) and ATC (20 μM). Accompanied by the red-to-purple color change of the solution and the corresponding fluorescence recovery, the detached RB molecules were monitored by HPLC via the emergence of a relatively lower monodisperse peak (trace 3) than that of trace 1 at the same elution time, demonstrating the partial detachment of RB molecules. In the presence of carbaryl, the peak almost disappeared (trace 4), indicating that no free RB molecules existed in the aqueous solution. More importantly, the amounts of free RB molecules could be quantified by calculating their peak areas from the HPLC analysis (Figure 2b).[44] The changes in the amounts of free RB molecules in solution confirmed the success of preparation of RB-AuNPs as well as the detection mechanism we proposed for this assay.

Sensitivity of This Assay for Pesticides. We next tested the sensitivity of this assay for carbaryl in aqueous solutions. To aliquots of AChE (10 milliunits/mL) solution were added various amounts of carbaryl (final concentrations were set to be 0, 0.1, 0.3, 0.6, 1.0, 3.0, 6.0, 10, and 100 μg/L). The mixtures were stored at 37 °C for 30 min. To each mixture was added RB-AuNPs (0.5 mL, 5 nM), and then aliquots of ATC (20 μM) were finally added into the mixtures. After 5 min of incubation, we found that the color of the solutions changed gradually from red to purple depending on the concentration of carbaryl. As the concentration of the pretreated carbaryl increased, the color of the solutions was darker red than those pretreated with lower concentrations of carbaryl. Figure 3a exhibits the concentration-dependent color changes, which were further confirmed by UV−vis absorption. With increasing concentrations of carbaryl, the absorption band at 520 nm increased gradually, along with the decreasing absorption band between 600 and 800 nm (Figure 3c). The plots of A_{520}/A_{700} (the ratio of absorbance at 520 and 700 nm) versus various concentrations of carbaryl reflected the linearly concentration-dependent process. Higher A_{520}/A_{700} values indicated lower degrees of aggregation of RB-AuNPs, corresponding to higher concentrations of carbaryl. In the meantime, the recovered fluorescence intensities of RB molecules were also based on the concentrations of carbaryl; that is, higher concentrations of carbaryl induced less fluorescence intensity (Figure 3b). We conclude that both the degree of color change of RB-AuNP solutions and their corresponding fluorescence recovery are proportional to the concentrations of carbaryl. The lowest detectable concentrations by the naked eye or fluorescence signal can be as low as 0.1 μg/L, which is much lower than those previously reported.[45−47]

To demonstrate that this dual-readout assay was functional not only for carbamate but also for organophosphorus compounds (the other main type of chemical pesticides in widespread use in real applications), we investigated the sensitivity of the sensing platform for three conventional organophosphorus compounds: diazinon, malathion, and phorate. The experimental procedures were the same as that

dx.doi.org/10.1021/ac300545p | Anal. Chem. 2012, 84, 4185−4191

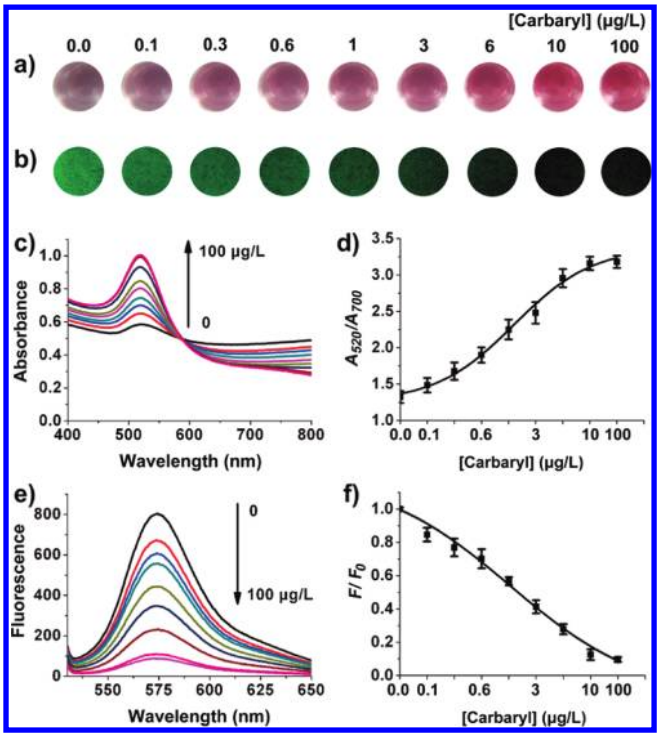

Figure 3. Sensitivity of this assay for carbaryl by color change and fluorescence recovery. (a) Color change with increasing concentrations of carbaryl from left to right (0–100 μg/L) and (b) corresponding fluorescence images of RB molecules. (c) Absorbance responses for panel a. (d) Plots of A_{520}/A_{700} values versus carbaryl concentrations. A_{520} indicated the absorption band at 520 nm, and A_{700} indicated the shoulder absorption band that appeared between 600 and 800 nm. (e) Fluorescence spectra for panel b and (f) their corresponding F/F_0 values versus different concentrations of carbaryl. The excitation wavelength was 550 nm. The fluorescence intensities were collected at 575 nm. The standard deviations of the samples were calculated for a sample size of 6.

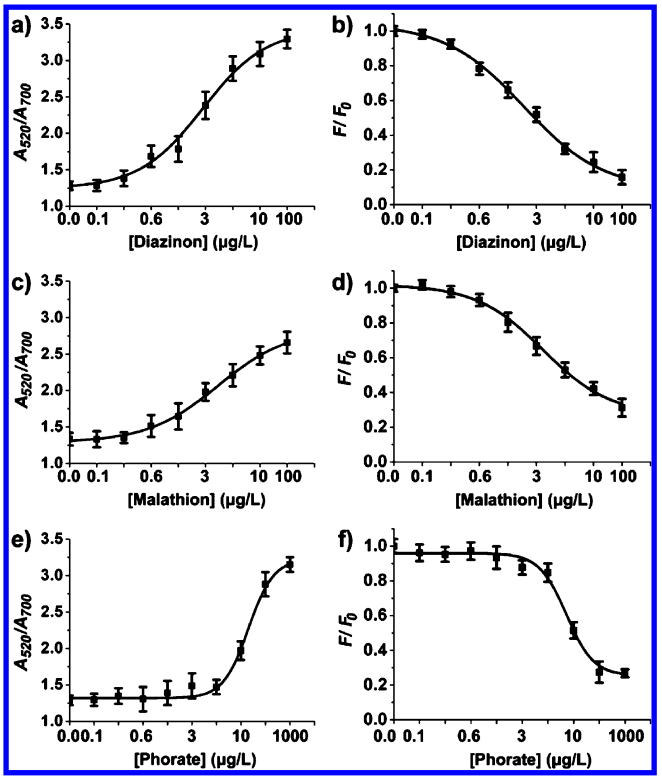

Figure 4. Plots of A_{520}/A_{700} values and their corresponding F/F_0 values versus different concentrations of pesticides. (a, b) Concentration-dependent inhibition responses of diazinon tested by UV–vis absorption and fluorescence variations, respectively; (c, d) those of malathion; (e, f) those of phorate. The standard deviations of the samples were calculated by a sample size of 6.

for carbaryl. We found that the inhibition responses were still dose-dependent. Figure 4a,c,e shows A_{520}/A_{700} values versus various concentrations of diazinon, malathion, and phorate, respectively. They had a similar trend to that of carbaryl. The apparent saturating inhibition concentrations for diazinon and malathion were found to be about 100 μg/L, while that for phorate was around 1000 μg/L. Moreover, their inhibition responses were monitored by testing the F/F_0 values (the ratio of fluorescence intensity at 575 nm in the presence and absence of pesticide) to various concentrations of the organophosphorus compounds. As shown in Figure 4b,d,f, with increasing pesticide concentrations, the fluorescence intensity diminished progressively, leading to the decrease of F/F_0 values. The lowest detectable concentrations for diazinon, malathion, and phorate are 0.1, 0.3, and 1 μg/L, respectively, which are much lower than the maximum residue limits (MRLs) as reported in the European Union pesticides database (MRLs are 0.05, 0.01, 0.02, and 0.05 ppm for carbaryl, diazinon, malathion, and phorate, respectively)[48] as well as that of United States (MRLs are 0.02, 0.02, and 0.02 ppm for carbaryl, malathion, and phorate, respectively; there are no data for diazinon).[49]

Inhibition Efficiencies of the Pesticides. From the color change and corresponding fluorescence responses, we could evaluate the inhibition efficiencies (IEs) of the above-mentioned pesticides as carbaryl > diazinon > malathion > phorate, which was further demonstrated by calculating the IC_{50} (the inhibitor concentrations where AChE activity was inhibited by 50%) value of each pesticide (Figure S4, Supporting Information). The IC_{50} values were obtained from the plots of IE versus concentration of pesticide. Similar to a previous report,[50] the IE values were calculated via eq 1, where C_0 represents the initial concentration of ATC and $C_{pesticide}$ and $C_{no\ pesticide}$ represent the concentrations of ATC during the hydrolysis reaction with AChE in the presence and absence of pesticides, respectively. On the basis of eq 1, the IC_{50} values for carbaryl, diazinon, malathion, and phorate were calculated to be 0.89, 1.93, 3.14, and 9.84 μg/L, respectively, indicating that carbaryl was the most potent inhibitor for blocking the activity of AChE among the four pesticides. On the basis of these findings, we suggest that this assay can be attractive to screen AChE inhibitors by UV–vis absorption or fluorescence spectra.

$$\mathrm{IE} = \frac{C_{\mathrm{pesticide}} - C_{\mathrm{no\ pesticide}}}{C_0 - C_{\mathrm{no\ pesticide}}} \times 100 \quad (1)$$

Detection of Carbaryl in Spiked Samples. As we reported in our previous work,[39] this enzyme-driven reaction-based assay has excellent specificity toward AChE. Because pesticides have very high efficiency in inhibiting AChE activities, we can anticipate that the matrices in real samples could have negligible interference with this assay for pesticides. To bring this assay into the real world, we next applied this dual-readout assay in monitoring pesticides in complex samples such as agricultural products and river water. River water and

dx.doi.org/10.1021/ac300545p | Anal. Chem. 2012, 84, 4185–4191

apple juice were spiked with varying levels of carbaryl to evaluate the effects of such sample matrices on detection. The final concentrations of carbaryl in the river water and apple juice were set to be 0, 0.01, 0.1, 1, 10, and 100 mg/L. The carbaryl in each spiked solution was monitored by using 5 μL of each sample to react with AChE (10 milliunits/mL) in 0.5 mL solutions containing RB-AuNPs (5 nM) and ATC (20 μM). We compared the inhibition plots of carbaryl in distilled water with those in spiked river water and apple juice. As shown in Figure 5, carbaryl in the three kinds of samples had similar

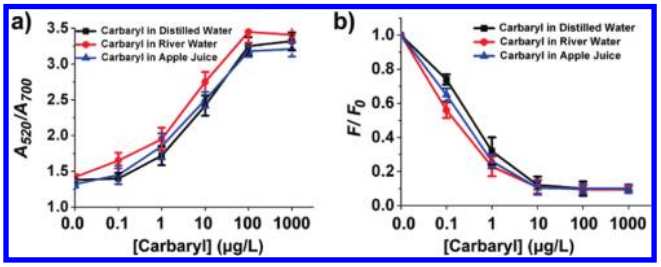

Figure 5. (a) Plots of A_{520}/A_{700} values and (b) their corresponding F/F_0 values versus different standard carbaryl concentrations in river water (red line) and apple juice (blue line), where the responses of absorption and fluorescence were similar to that in distilled water (black line). Standard deviations of the samples were calculated for a sample size of 6.

trends in absorption changes and fluorescence responses, which indicated that both the river water and apple juice matrices indeed had a negligible effect on detection limits and dynamic detection ranges. We conclude that this assay has the capability to sense pesticides in real samples. At this point, this method does not allow the researchers to tell one pesticide from another.

Determination of Carbaryl Residues with Time. Since pesticides are easily absorbed on the skins of agricultural products and their residues may cause fatal consequences, we evaluated whether the probe we described here could be utilized to monitor the residues of pesticides in food samples such as tomatoes and cucumbers. A standard carbaryl solution (100 mg/L) was sprayed on the skins of tomatoes and cucumbers, and the carbaryl residues in aliquots of the food samples were collected each day over the course of 1 week. We noticed that both the UV−vis absorption and fluorescence spectra had few changes for either carbaryl-sprayed tomatoes or cucumbers (Figure 6a,b), which indicated that the carbaryl residues on the skins of tomatoes and cucumbers remained stable for at least 1 week with negligible degradation. However, the levels of the carbaryl residues on the skins of tomatoes and cucumbers were different: the A_{520}/A_{700} values for tomatoes were lower than those for cucumbers, and the F/F_0 values for tomatoes were higher than those for cucumbers, indicating that the carbaryl residue levels on tomatoes were lower than those of cucumbers. The different carbaryl residues in real samples were clearly confirmed by HPLC. As shown in Figure 6c, we calculated the peak area for each sample from the HPLC analysis and found the amounts of carbaryl in either tomatoes or cucumbers indeed had negligible changes in 1 week, but the amounts of carbaryl in tomatoes were lower than those in cucumbers, indicating that carbaryl may absorb onto the skins of cucumbers more readily than those of tomatoes. To measure the amounts of carbaryl residues in tomato and cucumber samples, we established two calibration curves: one was based

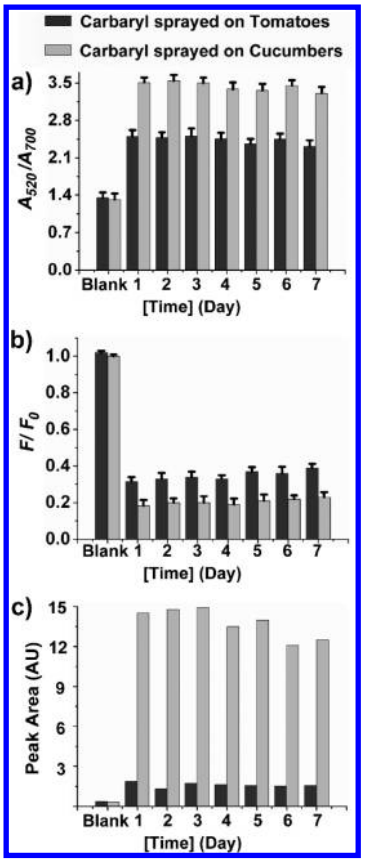

Figure 6. (a) A_{520}/A_{700} values and (b) their corresponding F/F_0 values for the carbaryl residues on the skins of tomatoes (dark gray bars) and cucumbers (light gray bars) in 1 week. (c) Amounts of carbaryl residues measured by HPLC analysis. The samples not sprayed with carbaryl were set as blank. Standard deviations of the samples were calculated for a sample size of 6.

on the absorbance signals and the other was based on the fluorescence signals (Figure S5, Supporting Information. By using the absorbance-based calibration curve, the amounts of carbaryl residues in tomato and cucumber samples were calculated to be 0.32 and 2.4 ppm, respectively; while they were calculated to be 0.25 and 1.7 ppm by use of the fluorescence-based calibration curve, respectively. These values are very close to those calibrated by HPLC analysis (0.23 and 2.2 ppm, respectively) (Figure S6, Supporting Information), demonstrating the validation of our dual-readout assay in the detection of pesticide residues in real samples.

In conclusion, we present a highly sensitive, dual-readout (colorimetric and fluorometric) assay for organophosphorus and carbamate pesticides. The detection mechanism was deeply investigated by using a variety of characterizations such as UV−vis absorption spectra, fluorescence spectra, ζ potential measurements, DLS, TEM images, and HPLC. The lowest detectable concentration for each pesticide by both the naked eye and fluorescence variations is much lower than the MRLs as reported in the European Union pesticides database as well as those from U.S. Department Agriculture. More importantly, we demonstrated the real-world application of this assay by detecting spiked pesticides in complex samples such as agricultural products and river water. We believe this assay can be useful in monitoring pesticides in most settings, especially in combination with other platforms such as lab-on-chip format.[51,52]

dx.doi.org/10.1021/ac300545p | *Anal. Chem.* 2012, 84, 4185−4191

■ ASSOCIATED CONTENT

Supporting Information

Six figures, as described in the text. This material is available free of charge via the Internet at http://pubs.acs.org.

■ AUTHOR INFORMATION

Corresponding Author

*E-mail: xingyujiang@nanoctr.cn or wangz@nanoctr.cn. Fax: (+86)10-82545631. Phone: (+86)10-82545611.

Notes

The authors declare no competing financial interest.

■ ACKNOWLEDGMENTS

D.L. and W.C. contributed equally to this work. We thank the Ministry of Science and Technology (2009CB30001, 2011CB933201, and 2012AA030608), the National Science Foundation of China (90813032, 20890023, 21025520, and 21105018), Beijing Natural Science Foundation (2122058), Youth Innovation Promotion Association, CAS, and the Chinese Academy of Sciences (KJCX2-YW-M15) for financial support.

■ REFERENCES

(1) http://www.who.int/foodsafety/publications/general/brochure_1999/en/index.html.
(2) Singh, S. K.; Tripathi, P. K.; Yadav, R. P.; Singh, D.; Singh, A. *Bull. Environ. Contam. Toxicol.* **2004**, *72*, 592−599.
(3) Jamal, G. A. *Toxicol. Rev.* **1997**, *16*, 133−170.
(4) de Solla, S. R.; Martina, P. A.; Mikodaa, P. *Sci. Total Environ.* **2011**, *409*, 4306−4311.
(5) Roast, S. D.; Thompson, R. S.; Donkin, P.; Widdows, J.; Jones, M. B. *Water Res.* **1999**, *33*, 319−326.
(6) Battaglin, W.; Fairchild, J. *Water Sci. Technol.* **2002**, *45*, 95−102.
(7) Dawson, A. H.; Eddleston, M.; Senarathna, L.; Mohamed, F.; Gawarammana, I.; Bowe, S. J.; Manuweera, G.; Buckley, N. A. *PLoS Med.* **2010**, *7*, No. e1000357.
(8) Mileson, B. E.; Chambers, J. E.; Chen, W. L.; Dettbarn, W.; Ehrich, M.; Eldefrawi, A. T.; Gaylor, D. W.; Hamernik, K.; Hodgson, E.; Karczmar, A. G.; Padilla, S.; Pope, C. N.; Richardson, R. J.; Saunders, D. R.; Sheets, L. P.; Sultatos, L. G.; Wallace, K. B. *Toxicol. Sci.* **1998**, *41*, 8−20.
(9) Pope, C. N. *J. Toxicol. Environ. Health B* **1999**, *2*, 161−181.
(10) Ray, D. E. *Toxicol. Lett.* **1998**, *102*, 527−533.
(11) Zimmerman, G.; Soreq, H. *Cell Tissue Res.* **2006**, *326*, 655−669.
(12) Lee, J.; Lee, H. K. *Anal. Chem.* **2011**, *83*, 6856−6861.
(13) Payá, P.; Anastassiades, M.; Mack, D.; Sigalova, I.; Tasdelen, B.; Oliva, J.; Barba, A. *Anal. Bioanal. Chem.* **2007**, *389*, 1697−1714.
(14) Viswanathan, S.; Radecka, H.; Radecki, J. *Biosens. Bioelectron.* **2009**, *24*, 2772−2777.
(15) Liu, G. D.; Lin, Y. H. *Anal. Chem.* **2005**, *77*, 5894−5901.
(16) Yong, D. M.; Liu, C.; Yu, D. B.; Dong, S. J. *Talanta* **2011**, *84*, 7−12.
(17) Qian, G. L.; Wang, L. M.; Wu, Y. R.; Zhang, Q.; Sun, Q.; Liu, Y.; Liu, F. Q. *Food Chem.* **2009**, *117*, 364−370.
(18) Jain, P. K.; Huang, X. H.; El-Sayed, I. H.; El-Sayed, M. A. *Acc. Chem. Res.* **2008**, *41*, 1578−1586.
(19) Katz, E.; Willner, I. *Angew. Chem., Int. Ed.* **2004**, *43*, 6042−6108.
(20) Song, S. P.; Qin, Y.; He, Y.; Huang, Q.; Fan, C. H.; Chen, H. Y. *Chem. Soc. Rev.* **2010**, *39*, 4234−4243.
(21) Liu, D. B.; Wang, Z.; Jiang, X. Y. *Nanoscale* **2011**, *3*, 1421−1433.
(22) Zheng, Z. Z.; Zhou, Y. L.; Li, X. Y.; Liu, S. Q.; Tang, Z. Y. *Biosens. Bioelectron.* **2011**, *26*, 3081−3085.
(23) Asensio-Ramos, M.; Hernandez-Borges, J.; Borges-Miquel, T. M.; Rodriguez-Delgado, M. A. *Anal. Chim. Acta* **2009**, *647*, 167−176.
(24) Su, Y. Y.; Peng, F.; Jiang, Z. Y.; Zhong, Y. L.; Lu, Y. M.; Jiang, X. X.; Huang, Q.; Fan, C. H.; Lee, S. T.; He, Y. *Biomaterials* **2011**, *32*, 5855−5862.
(25) Fischer, H. C.; Liu, L. C.; Pang, K. S.; Chan, W. C. W. *Adv. Funct. Mater.* **2006**, *16*, 1299−1305.
(26) Cho, S. J.; Maysinger, D.; Jain, M.; Roder, B.; Hackbarth, S.; Winnik, F. M. *Langmuir* **2007**, *23*, 1974−1980.
(27) Liu, S. Q.; Yuan, L.; Yue, X. L.; Zheng, Z. Z.; Tang, Z. Y. *Adv. Powder Technol.* **2008**, *19*, 419−441.
(28) Elghanian, R.; Storhoff, J. J.; Mucic, R. C.; Letsinger, R. L.; Mirkin, C. A. *Science* **1997**, *277*, 1078−1081.
(29) Liu, J. W.; Lu, Y. *J. Am. Chem. Soc.* **2003**, *125*, 6642−6643.
(30) Huang, C. C.; Huang, Y. F.; Cao, Z. H.; Tan, W. H.; Chang, H. T. *Anal. Chem.* **2005**, *77*, 5735−5741.
(31) Wang, L. H.; Liu, X. F.; Hu, X. F.; Song, S. P.; Fan, C. H. *Chem. Commun.* **2006**, *36*, 3780−3782.
(32) Liu, D. B.; Qu, W. S.; Chen, W. W.; Zhang, W.; Wang, Z.; Jiang, X. Y. *Anal. Chem.* **2010**, *82*, 9606−9610.
(33) Nam, J. M.; Wise, A. R.; Groves, J. T. *Anal. Chem.* **2005**, *77*, 6985−6988.
(34) Klajn, R.; Stoddart, J. F.; Grzybowski, B. A. *Chem. Soc. Rev.* **2010**, *39*, 2203−2237.
(35) Sun, J.; Guo, L.; Bao, Y.; Xie, J. *Biosens. Bioelectron.* **2011**, *28*, 152−157.
(36) Virel, A.; Saa, L.; Pavlov, V. *Anal. Chem.* **2009**, *81*, 268−272.
(37) Li, H. K.; Guo, J. J.; Ping, H.; Liu, L. R.; Zhang, M. W.; Guan, F. R.; Sun, C. Y.; Zhang, Q. *Talanta* **2011**, *87*, 93−99.
(38) Xu, Q.; Du, S.; Jin, G. D.; Li, H. B.; Hu, X. Y. *Microchim Acta* **2011**, *173*, 323−329.
(39) Liu, D. B.; Chen, W. W.; Tian, Y.; He, S.; Zheng, W. F.; Sun, J. S.; Wang, Z.; Jiang, X. Y. *Adv. Healthcare Mater.* **2012**, *1*, 90−95.
(40) Liu, D. B.; Chen, W. W.; Sun, K.; Deng, K.; Zhang, W.; Wang, Z.; Jiang, X. Y. *Angew. Chem., Int. Ed.* **2011**, *50*, 4103−4107.
(41) Shang, L.; Jin, L. H.; Dong, S. J. *Chem. Commun.* **2009**, *21*, 3077−3079.
(42) Valdes-Ramirez, G.; Cortina, M.; Ramirez-Silva, M. T.; Marty, J. L. *Anal. Bioanal. Chem.* **2008**, *392*, 699−707.
(43) Du, D.; Wang, M. H.; Cai, J.; Tao, Y.; Tu, H. Y.; Zhang, A. D. *Analyst* **2008**, *133*, 1790−1795.
(44) Spivak, W.; Carey, M. C. *Biochem. J.* **1985**, *225*, 787−805.
(45) Hossain, S. M. Z.; Luckham, R. E.; McFadden, M. J.; Brennan, J. D. *Anal. Chem.* **2009**, *81*, 9055−9064.
(46) Wang, K.; Liu, Q.; Dai, L.; Yan, J. J.; Ju, C.; Qiu, B. J.; Wu, X. Y. *Anal. Chim. Acta* **2011**, *695*, 84−88.
(47) Pedrosa, V. A.; Caetano, J.; Machado, S. A. S.; Bertotti, M. *Sensors* **2008**, *8*, 4600−4610.
(48) http://ec.europa.eu/sanco_pesticides/public/index.cfm.
(49) http://www.mrldatabase.com/default.cfm?selectvetdrug=0.
(50) Feng, F. D.; Tang, Y. L.; Wang, S.; Li, Y. L.; Zhu, D. B. *Angew. Chem., Int. Ed.* **2007**, *46*, 7882−7886.
(51) Yang, D. Y.; Niu, X.; Liu, Y. Y.; Wang, Y.; Gu, X.; Song, L. S.; Zhao, R.; Ma, L. Y.; Shao, Y. M.; Jiang, X. Y. *Adv. Mater.* **2008**, *20*, 4770−4775.
(52) Zhang, W.; Lin, S.; Wang, C.; Hu, J.; Li, C.; Zhuang, Z.; Zhou, Y.; Mathies, R. A.; Yang, C. J. *Lab Chip* **2009**, *9*, 3088−3094.